

REPORT DOCUMENTATION PAGE

AFRL-SR-BL-TR-98-

0849

Public reporting burden for this collection of information is estimated to average 1 hour per response, including gathering and maintaining the data needed, and completing and reviewing the collection of information. Send collection of information, including suggestions for reducing this burden, to Washington Headquarters Services, Directorate for Information Operations and Reports, 1215 Jefferson Davis Highway, Suite 1204, Arlington, VA 22202-4302, and to the Office of Management and Budget, Paperwork Project, Washington, DC 20503.

BS,
his
on

1. AGENCY USE ONLY (Leave blank)		2. REPORT DATE	3. REPORT TYPE AND DATES COVERED 01 Sep 97 to 31 Aug 98 (Final)	
4. TITLE AND SUBTITLE Str-97 A DC Steady current atmospheric discharge for battlefield CHEM/BIO Decontamination			5. FUNDING NUMBERS 65502f STTR/TS	
6. AUTHOR(S) Dr Kim				
7. PERFORMING ORGANIZATION NAME(S) AND ADDRESS(ES) Plasmion corporation 50 Harrison Street Hoboken NJ 07030			8. PERFORMING ORGANIZATION REPORT NUMBER	
9. SPONSORING/MONITORING AGENCY NAME(S) AND ADDRESS(ES) AFOSR/NE 801 North Randolph Street Rm 732 Arlington, VA 22203-1977			10. SPONSORING/MONITORING AGENCY REPORT NUMBER F49620-97-C-0073	
11. SUPPLEMENTARY NOTES 19990104 008				
12a. DISTRIBUTION AVAILABILITY STATEMENT APPROVAL FOR PUBLIC RELEASE; DISTRIBUTION UNLIMITED			12b. DISTRIBUTION CODE	
13. ABSTRACT (Maximum 200 words) In this Phase 1, A Capillary Plasma Electrode Discharge (CPED) test system was designed and constructed using a vacuum system equipped with three mass flow controllers (MFC) and a linear motion manipulator. In order to compare our CPED with other conventional ac-barrier type discharge, we tested CPED and ac-barrier type arrangement discharge. The complete characteristics of the CPED and ac-barrier type discharge have been analyzed. Reproduced From Best Available Copy				
14. SUBJECT TERMS			15. NUMBER OF PAGES	
			16. PRICE CODE	
17. SECURITY CLASSIFICATION OF REPORT UNCLASSIFIED	18. SECURITY CLASSIFICATION OF THIS PAGE UNCLASSIFIED	19. SECURITY CLASSIFICATION OF ABSTRACT UNCLASSIFIED	20. LIMITATION OF ABSTRACT UL	

Final Technical Report

Item No: 0002AA

Title of the Project:

A DC Steady Current Atmospheric Pressure Discharge
for Battlefield Chem/Bio Decontamination

Topic No.:	AF 97T002
Proc Instrument ID No.:	F49620-97-C-0073
Contract Starting Date:	September 1, 1997
Contract Ending Date:	August 31, 1998
Contractor:	PLASMION Corporation 50 Harrison Street Hoboken, NJ 07030

Prepared By:

Dr. Steven Kim

Principal Investigator

PLASMION Corporation

Report Date: November 30, 1998

CONTENT

1. Abstract	2
2. Summary of Phase I Accomplishments	4
CPED Shower and decontamination capability	5
3. Introduction	6
4. Significance of CPED	10
Physics of CPED	10
5. Phase I Performance	16
5-1. Statement of Work - Accomplishments	16
5-2. Investigation of Optimum d/L Ratio of CPED Electrodes	17
5-3. Apparatus and Process	18
5-4. Experimental Results	22
5-5. Conclusion	36
6. Phase II Plan	37
Overview	37
Refine the process technology	38
Construct a portable 6" CPED Shower	39
Field work of decontamination	40
7. References	44

1. Abstract

Recently, several researchers demonstrated the feasibility of high (atmospheric) pressure glow discharge (HPGD) for various practical applications. However, most of them utilize high voltage pulses ($> 5\text{kV rms}$), which is not desirable in practical applications for many reasons. Kunhardt et al at Stevens Institute of Technology has invented a novel mechanism to generate a stable HPG discharge. The basis of this approach is the suppression of the glow-to-arc transition instability by creating a self-stabilizing cathode fall and thereby preventing the formation of a cathode spot. This is achieved simply by placing a perforated thin dielectric on the cathode surface. Due to the unique current limiting mechanism of a micro-channel, one can actually maintain the discharge in a steady current mode. Thus, the reactive radicals and ions would be much more power effective for decontamination.

In this Phase I, A Capillary Plasma Electrode Discharge (CPED) test system was designed and constructed using a vacuum system equipped with three mass flow controllers (MFC) and a linear motion manipulator. In order to compare our CPED with other conventional ac-barrier type discharge, we tested CPED and ac-barrier type arrangement discharge. The complete characteristics of the CPED and ac-barrier type discharge have been analyzed.

We investigated the discharge characteristics as functions of frequency and voltage for various types of barrier dielectric plates. By controlling the frequency, we were able to change the discharge mode from a capillary mode (with enhanced plasma density and U-V photon) to diffuse mode (ac barrier type). The capillary mode has been found to be stable in between 70-150 kHz range. The dimensions of the optimum perforated dielectric was investigated using two different d/L ratio (1/5 and 1/10) capillary electrodes. We made a portable decontamination shower with a $\frac{1}{2}$ inch diameter beam using CEDP. We investigated the treatment of bacteria by capillary and diffuse plasmas. Perfect pasteurization of bacteria was only possible using the capillary mode plasma, despite the fact that the power used was much lower than that of the diffuse plasma.

We designed a test chamber with a 6-inch diameter plasma and a portable plasma shower with a 6 inch beams which will be developed in Phase II. A prototype field-portable atmospheric pressure glow discharge plasma decontamination system will be fabricated and used to demonstrate the full capability of decontamination against realistic bio/chemical warfare agents.

2. Summary of Phase I Accomplishments

PLASMION has invented and developed a Capillary Plasma Electrode Discharge (CPED) Showerhead for chem/bio decontamination. The device is based on an invention, Method and Apparatus for Suppression of the Glow-to-Arc Transition, of Prof. E. E. Kunhardt from Stevens Institute of Technology.

A major technique for the generation of atmospheric pressure plasma has been the AC barrier discharge, operated either in the diffuse or micro-discharge modes. In this type of discharge, a dielectric layer is used to prevent the transition to the high current arc discharge; however, its high voltage and low plasma density are critical drawbacks for wide commercial applications.

PLASMION's CPED innovation may be viewed as a technique for enhancing the characteristics of the barrier discharge. That is, by perforating the dielectric layer with capillary holes, we can obtain higher plasma density, lower sustaining voltages, and a longer conduction period per AC cycle. Moreover, the CPED can also be operated in a pulsed DC mode, which places less demand on the power supply. CPED has significantly higher plasma density than the conventional AC barrier type discharge at less than half of the discharge voltage as shown in Fig. 2-1.

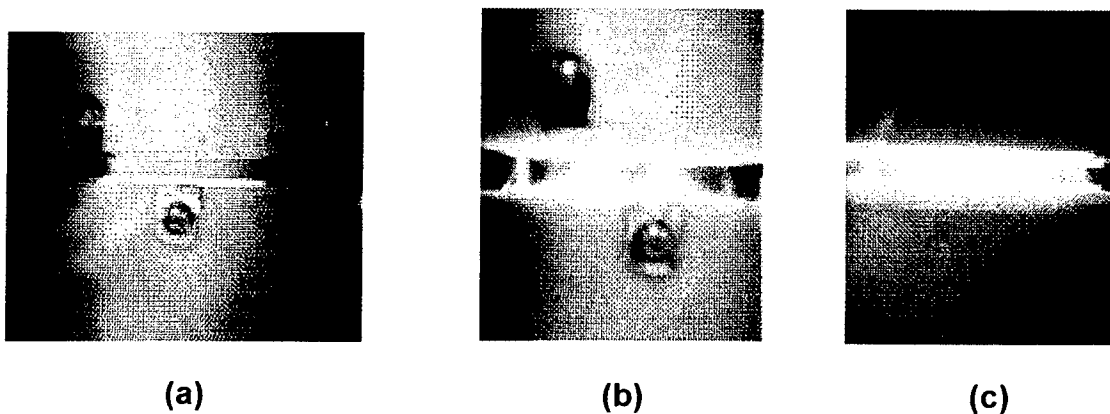
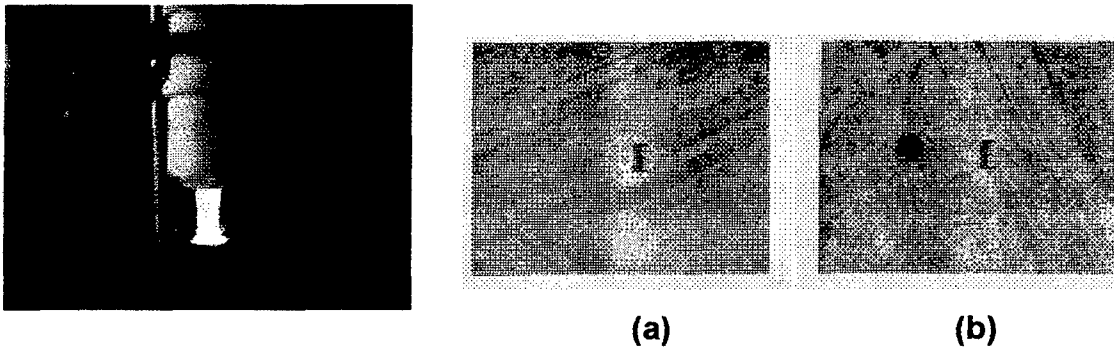


Fig. 2-1 Comparison between (a) AC barrier type and (b) & (c) CPED

CPED Shower and decontamination capability

Due to the versatile structure of the CPED, we successfully developed a CPED shower – cold plasma spray – which is ideal for outdoor decontamination applications as shown in Fig. 2-2. We performed a decontamination test to compare how effectively the AC barrier-type and CPED destroy microorganisms. Our test shows that although the conventional barrier discharge reduced microbial viability, it did not destroy all the microbes. With the CPED, however, we were able to efficiently destroy all microbes, including highly resistant spore-forming microbes from the genus that includes the deadly anthrax bacterium.



**Fig. 2-2 CPED Shower and image of (a) CPED treated: no bacteria growth
(b) AC barrier type treated: microbial growth observed.**

3. Introduction

A stabilized high (atmospheric) pressure DC glow discharge (HPG) was first reported in 1927 by Wehrli. [1] The discharge volume was typically less than one cm³.

Stable RF HPG demonstrated by Okazaki and co-workers in Japan, [2] and later by Roth and co-workers in the USA [3] as shown in Fig. 3-1 (a) and (b). The RF frequency is typically in the kHz range (although the Japanese group has gone as low as 50 Hz). Stabilization is achieved by arresting the development of the breakdown process; i.e. terminating the discharge before the onset of the glow-to-arc transition. This is implemented by placing insulators in front of the electrodes. The insulator in front of the electrode acting as anode during the RF cycle charges up negatively, thereby canceling the applied field and terminating the ionization growth. This process occurs every half cycle. Thus, the "discharge" is actually a series of self-arrested "pulsed" HPG, two per cycle. Typical current pulses from the work by Okazaki and by Roth are shown at right. Note that there is approximately a 200 μ s window between discharge pulses. In an attaching gas (such as atmospheric air), the electron density during this quiescent period may drop to practically zero. Therefore, these plasma have a low duty cycle so that the contaminated items have a limited exposure as compared to a DC plasma.

It may be possible to reduce the duration of the quiescent period by increasing the frequency of the RF. However, this has the effect of increasing the breakdown voltage (since the electron space charge begins to affect the breakdown process). For these conditions, the gain per avalanche (at high pressure) is sufficient to cause the formation of streamers and consequently breakdown is of the filamentary type (similar to a barrier discharge). It is no longer possible to generate the glow phase.

Large volume DC plasmas at atmospheric pressures have recently been demonstrated by Akishev *et. al.* [4] The scheme of the experiment shown in Fig. 3-1 (c). Plasma stability was achieved by using a multiple pin cathode, with each pin resistively ballast (1 mW per pin). These discharges are essentially a number

of "small volume" HPGs operated in parallel. The separation between the HPG is of the order of mm so that they merge into a volume glow. The large power dissipation in the ballast resistors makes this approach highly inefficient.

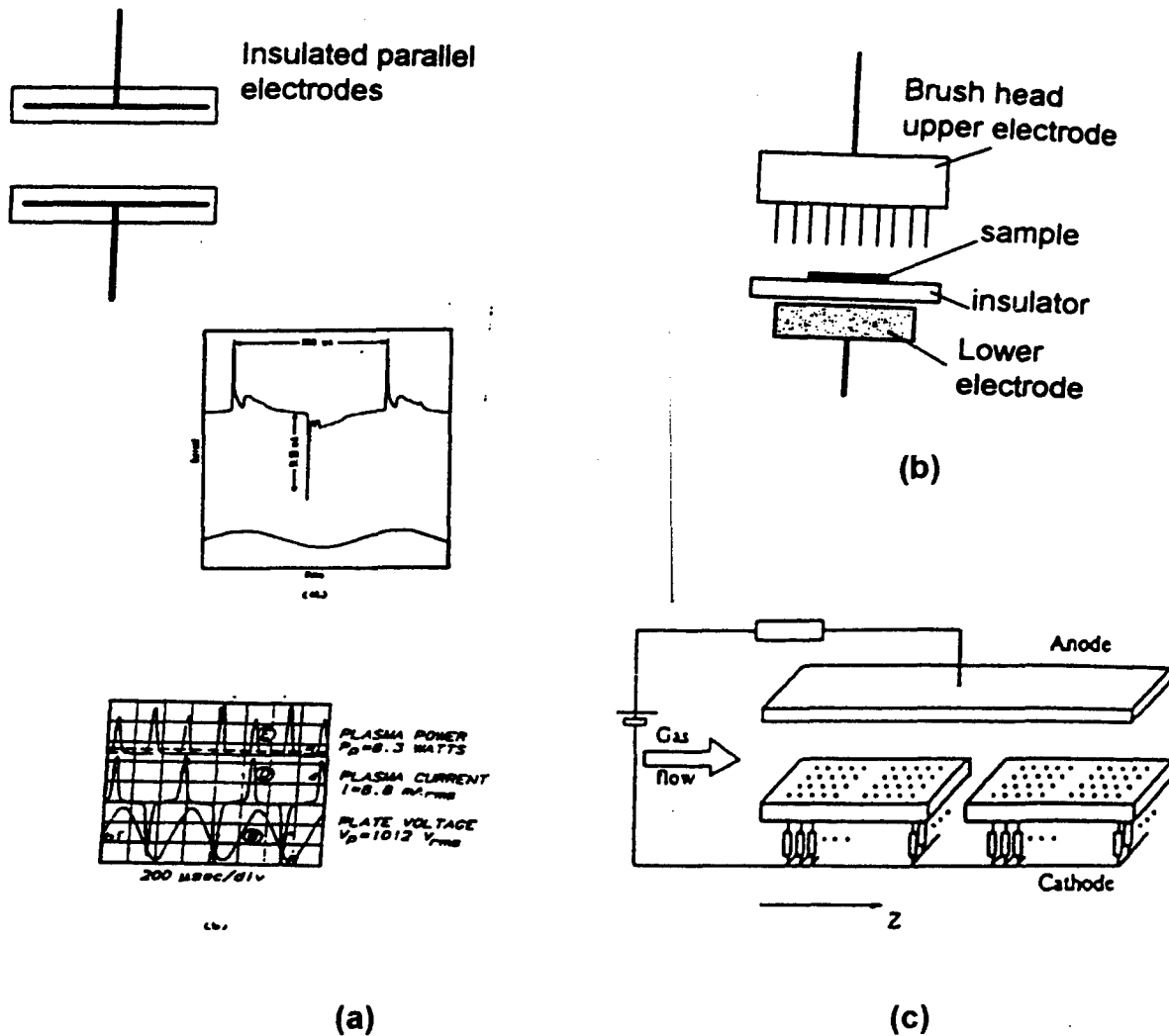


Fig. 3-1 Scheme of plasma systems in previous studies. [2,3,4]

In air the main electron loss process is electron attachment to oxygen. The energy density required to sustain a discharge in such an attaching gas is given by:

$$P = n_e W_{\text{ion}}/\tau$$

where n_e is the electron density, W_{ion} the effective ionization energy, and τ is the average lifetime of the electrons. At concentrations of 10^{10} cm^{-3} , in atmospheric air, τ is 10 ns. [5] Assuming that the effective ionization energy is 50 eV, the power density required for the sustenance of an atmospheric air plasma with an electron density of 10^{10} cm^{-3} is 8 W/cm^3 .

The electron losses due to attachment which lead to large energy consumption, may be drastically reduced by heating the air to temperatures on the order of 2,000 K. This can be achieved with the discharge current. The attaching air is, by this process converted into a quasi-non-attaching gas mixture, can be estimated by considering noble gases. In noble gases, where attachment is negligible, the electron lifetime is orders of magnitude longer than that in air, the power required to sustain a discharge is correspondingly much lower. This power density is given as:

$$P = k n_e^2 W_{\text{ion}}$$

where k is the rate coefficient for two-body recombination. The rate coefficient for dissociative recombination, which is assumed to be dominating recombination process, is e.g. for He, $10^{-8} \text{ cm}^3/\text{s}$. The required energy to sustain a plasma with 10^{10} cm^{-3} in He is therefore 8 mW/cm^3 , three orders of magnitude below the value for atmospheric air. This simple calculation gives us an indication of the energy savings when attachment is removed as an energy loss process. These effects can be used to fine tune the overall efficiency of the system for field application.

Much of the efforts in generating stable glow discharge at high pressure in both dc and RF discharges [6] have focused on preventing the onset of instabilities in the region near the electrodes, for dc discharges particularly in the cathode region. These are the regions of higher electric field and consequently higher power density compared to the positive column of the discharge. This region is therefore the cradle of instabilities which lead to constrictions and arc

formation in the discharge. Segmentation of the cathode, and ballasting the individual discharges resistively has been used to prevent the onset of glow to arc instability in atmospheric pressure air glow discharges. [7] The self-stabilized perforated dielectric effectively prevents this transition in a similar manner. Each of micro holes acts as a separate, active-current-limiting micro-channel.

The key issue in the generation of non-thermal atmospheric pressure discharges is how to prevent the glow-to-arc transition. The conventional approach is to cover the electrodes with a dielectric layer so that the discharge terminates when the capacitance of the layer is fully charged. This is designed to occur before the transition into the high current arc. By using an ac source, a continuous train of discharge pulses are obtained with the electrodes reversing their role in each half-cycle. This type of discharge has several limitations for a wide range of applications: (1) Since both of the electrodes are covered by an insulator, DC or pulsed DC (i.e. train of unipolar pulses) steady state operation is not possible. DC or pulsed DC steady state operation is desirable for high duty factor operation. (2) Inefficient operational conditions: The conventional AC barrier type utilize a dielectric layer and more than half of the potential can be dropped across this layer. This implies the need for higher applied voltage to breakdown the gas and also results in a low plasma density. This is not just an inefficiency, but it directly relates to the economics and portability of the approach (reflected in power supply and insulator requirements). (3) Limitation in structure: In order to be used in a battlefield application, the plasma source should be portable and applicable to various size and shapes of targets. It is difficult to engineer a sizable spray type plasma source based on barrier discharge. (4) Low density plasma: AC barrier type operation produces a low density plasma, which we have shown not to be sufficient for killing some spore forming bacteria.

The CPED overcomes all these limitations. In this report, we describe how CPED solves these technical difficulties and demonstrate the CPED concept at atmospheric pressure. We present the experimental results, its superior bacteria and spore destruction capacity over conventional barrier discharges, and developed a portable shower concept.

4. Significance of CPED

Physics of CPED

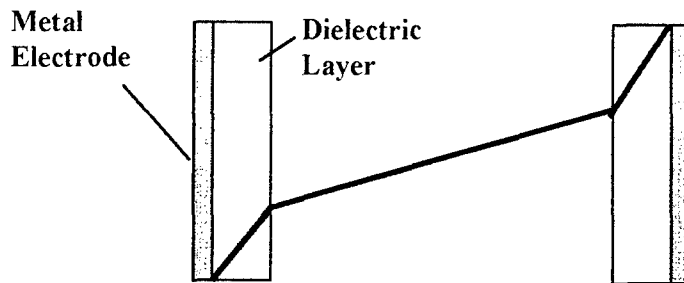
The physics of an ac barrier discharge operating in the micro-discharge mode is now well understood (Kogelshatz et. al. 1997). This is not the case for the diffuse mode of operation. Although a number of laboratories have now demonstrated this mode of operation (Okazaki et. al. In Japan, [2] the first to observe this discharge mode, Massiness et. al. in France [8], Roth et. al. [3] and Kunhardt et. al. in the US), a number of issues remain unexplained. Among these issues are: 1) the boundary conditions at the dielectric layers that lead to discharge uniformity and 2) the conditions in the bulk that lead to a modification of the Townsend ionization coefficient, α . These conditions permit the ignition of the discharge each half cycle at voltages below that needed to breakdown the quiescent gas.

It is however possible to provide a qualitative picture of the discharge dynamics during a half cycle of a barrier discharge operating in the diffuse mode. This is shown in Fig. 4-1. The frequency of stable operation lies in the regime of 1-200 kHz, depending on the electrode characteristics. The potential distribution between the electrodes as the voltage increases is shown in Fig. 4-1 (b). Note the higher field across the dielectric layers. The subsequent generation of electron avalanches in the bulk, with the concomitant generation of U-V radiation, lead to space-charge formation and collapse of the voltage between the dielectric layers as well as a shift in the spectral emission to the visible. This is also accompanied by the further charging of the capacitance represented by the dielectric layers, as shown by the increase in the slope of the voltage in Fig. 4-1 (c), and finally, to the arrest of the discharge. It is not possible with this approach to obtain a period of conduction longer than that required to charge this capacitance at the operating conditions.

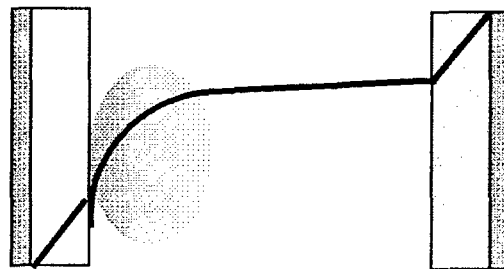
To obtain another discharge pulse, it is necessary to re-establish the field between the dielectric layers by reversing the polarity of the applied field (thus ac operation) and retracing the process outlined above. In this fashion, a series of

discharge pulses of limited duration are obtained, one every half cycle, with the electrodes reversing their role as either cathode or anode.

(a) Potential distribution before the ignition of discharge



(b) Potential distribution in ignition transient period



(c) Potential distribution in the steady state discharge

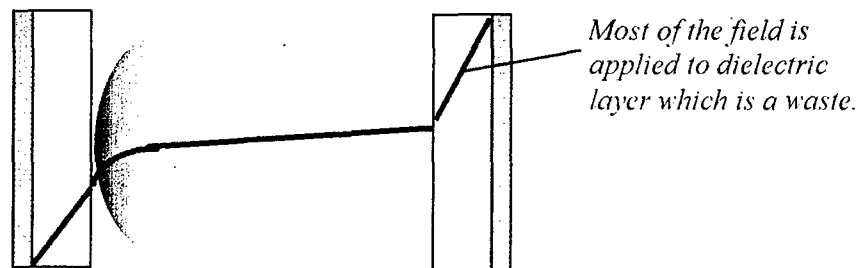


Fig. 4-1 Schematic presentation of the evolution of the potential across an AC barrier discharge.

In the CPED concept, the dielectric layer is perforated with capillary holes, whose density and diameter can be varied in order to optimize the discharge characteristics depending on the application. This simple change in electrode configuration results in a number of advantages:

1. Since conduction to the metal electrode is permitted, the duration of the discharge pulse during a half cycle is not determined by the barrier capacitance but by the operating frequency.
2. By permitting the barrier capacitance to discharge in every half cycle, it is possible to operate the discharge with uni-polar pulses, that is pulsed DC. This provides additional degrees of freedom since the duty factor of the applied voltage can be varied depending on the application. Moreover, it simplifies the development of a high voltage, portable power supply for battlefield applications.
3. The large field that appears across the dielectric layer in the early phase of a cycle can be used to generate electron avalanches in the capillary, which facilitate the breakdown of the gap.
4. Since the field in the capillary does not collapse, as does the field in the bulk, a streamer discharge is maintained in the capillary, which results in larger plasma densities in the bulk as well as enhanced U-V production. These two factors contribute to the better killing performance of the CPED vs. the conventional ac barrier discharge.

Figure 4-2 shows the potential distribution in CPED structure. The high electric field maintained in the capillary in the dielectric layer that produces high-density plasma. These features of the CPED are qualitatively illustrated in Fig. 4-3. (a) in Fig. 4-3 illustrates the field inside the capillary hole leading to the development of a streamer discharge starting from the metal electrode, as shown in Fig. 4-2 (b). The high-density plasma in the capillary emerges from the end of the capillary into the gap where it serves as electrode for the main discharge. The field inside the capillary does not collapse after the formation of the streamer discharge. This is due to the fact that high electron-ion recombination at the wall

requires a large production rate on axis (and therefore a high field), in order to sustain the current. At the interface of the capillary plasma and the main discharge a double layer is expected to exist, as occurs for example in the grid holes of a thyratron switch (Penetrante and Kunhardt, 1988).

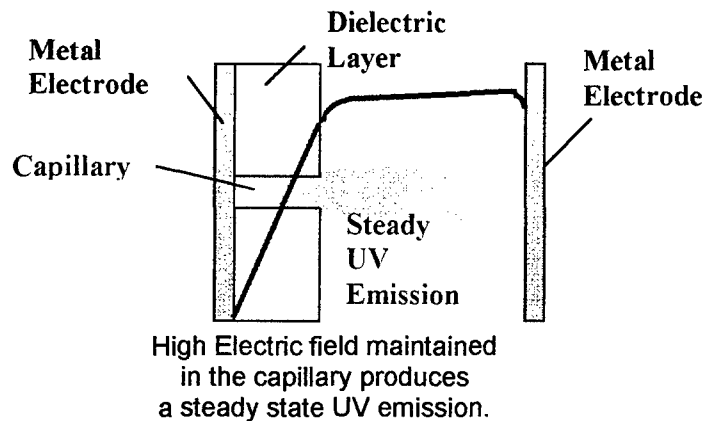
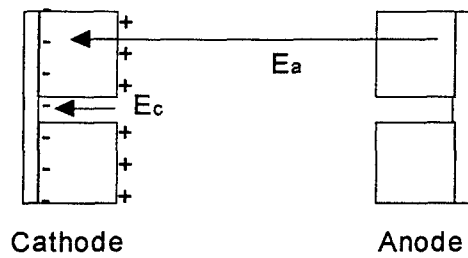
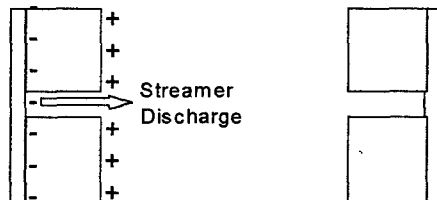


Fig. 4-2 Schematic of Potential distribution in CPED Structure.

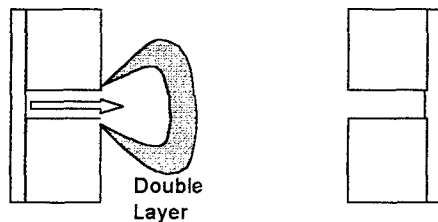
An experimental demonstration of this phenomenon is shown in Fig. 4-4. By properly choosing the ratio of d , the diameter of the capillary, to L , the length of the capillary tube, a steady state can be sustained, as shown in Fig. 4-3 (c). The anode need not be covered with a dielectric layer if uni-polar operation is desired. The efficiency of the capillary plasma as electrode results in a lower sustaining voltage for the main discharge. This has been verified experimentally. Runaway into the arc is prevented by the fact that the current through the capillary is self-limiting. That is, since the gas density inside the capillary decreases with time due to Joule energy heating, there is an upper limit to the conductivity as result of gas starvation (unlike an open channel, there is no new source of neutrals inside the capillary). If larger currents are demanded to pass through the capillary, the conduction is disrupted. This phenomenon is also observed in thyratron switches due to the presence of grid hole (Penetrante and



- (a) Electric field in the capillary, E_c , and applied field, E_a , in the starting phase of a half cycle.



- (b) Streamer discharge forms in the capillary. The field in this region does not collapse due to large electron-ion recombination at the wall.

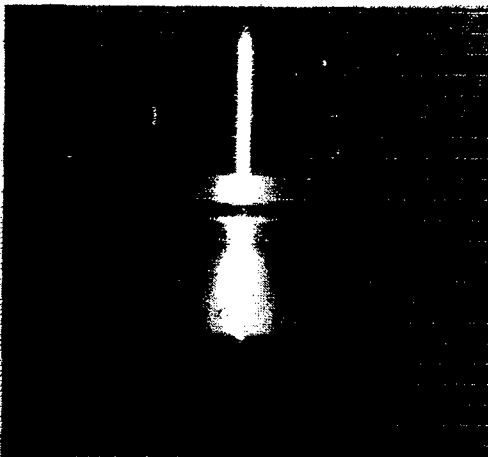


- (c) In steady state, a double layer forms between high density capillary plasma and main discharge plasma. The capillary plasma serves as electrode for the main discharge

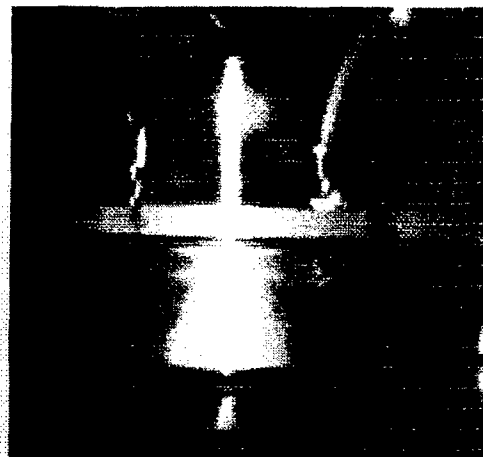
Fig. 4-3 Schematic presentation CPED.

Kunhardt, 1988). Thus, the ratio d/L can be chosen for a suitable duty cycle of operation. This is one of our main topic of investigation at this time.

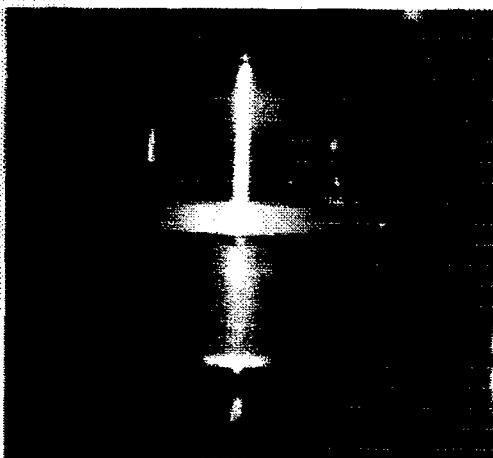
(a)



(d)



(b)



(c)

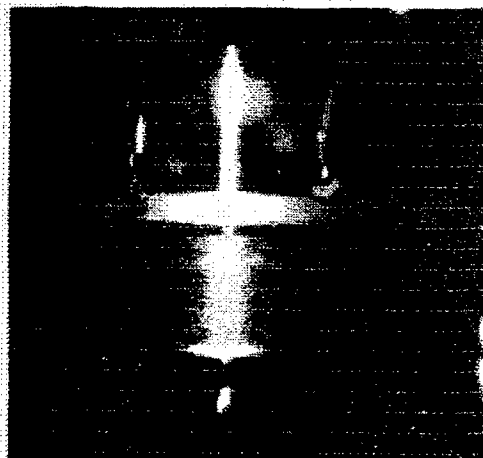


Fig. 4-4 Photos of Capillary Electrode Discharge at 30 Torr, increasing currents from (a) to (d).

5. Phase I Performance

5-1. Statement of Work – Accomplishments

1. Design & construction of the HPGD beam source Month: 0-3 Completed

The HPGD system was designed and constructed using a vacuum system, whose pressure can be controlled from 10 mTorr to 760 Torr, which was equipped with three mass flow controllers (MFC) and a linear motion manipulator.

2. Development of the optimum perforated dielectric cathode Month: 0-8 Completed

The dimensions of the optimum perforated dielectric was investigated using two different d/L ratio (1/5 and 1/10) capillary electrodes in our experimental condition.

3. Characterization of the source Month: 4-9 Completed

We studied characterization of plasma by varying AC frequency, power, distance of electrode, and type of CPED in He atmosphere.

4. Evaluation of the decontamination capability Month: 5-10 Completed

We demonstrated the decontamination capability by subjecting samples to conventional AC barrier type discharge and CPED discharge.

5. Design a field portable system Month: 9-12 Completed

Based on optimized conditions for the CPED structure, we designed a portable CPED Shower.

6. Submit a final report Month: 12 Completed

5-2. Investigation of Optimum d/L Ratio of CPED Electrodes

We have developed a MonteCarlo code for simulating the development of the streamer discharge inside a capillary tube. This code takes into account the more important electron-neutral collision processes (there is no intrinsic limitation as to the number of processes), electron-ion interactions (including space-charge fields), interactions between electrons, ions, and neutrals and the capillary wall, as well as electron-ion recombination in the bulk and at the wall. This code is derived from the code used by Tzeng and Kunhardt (1988) to simulate bulk streamers in gases (including electronegative gases) under the action of uniform external fields. The code is at present fully operational, and preliminary results have been obtained for rare gases (He, Ar, Xe). Our objective is to extend it to pure air or air mixtures (the mixtures to be considered will be functions of what is deemed to be best for killing particular spores). Using this code, we can:

- 1) investigate the charge buildup inside the capillary as a function of capillary radius,
- 2) determine the density at the exit of the capillary as a function of capillary length,
- 3) determine the applied field required to initiate the breakdown process,
- 4) calculate the photon yield of the streamer discharge, and
- 5) determine the density of capillaries necessary to obtain overlap of the exit discharge plasma.

Investigations for the optimum d/L ratio of these capabilities have been carried out on a new type of electrical discharge in a gas between high density plasma electrodes. The plasma forming the electrode is generated in capillary tubes placed in front of and with axis perpendicular to plane metal electrodes (see Fig. 4-2). A single capillary has diameter, D , ranging from 5 μm to 0.25 mm and length, L , to diameter ratio (L/D) of the order of 100. The diameter of the plasma electrode is determined by the number of capillaries that are combined in parallel, as well as by their separation. Experiments have been conducted with

single, four, and 100,000 capillary electrodes. Thus far, we have only used these electrodes as cathodes. There are no limitations on also using them as anode. The experiments with single and four capillary cathodes have been conducted with DC excitation at pressures 760 Torr.

5-3. Apparatus and Process

We constructed the test system as shown in Fig. 5-1. The system has a capability to insert various dielectric electrodes with capillaries of different d/L ratios, changing the gap distance between the electrodes, changing the operational pressure, and combination of gases.

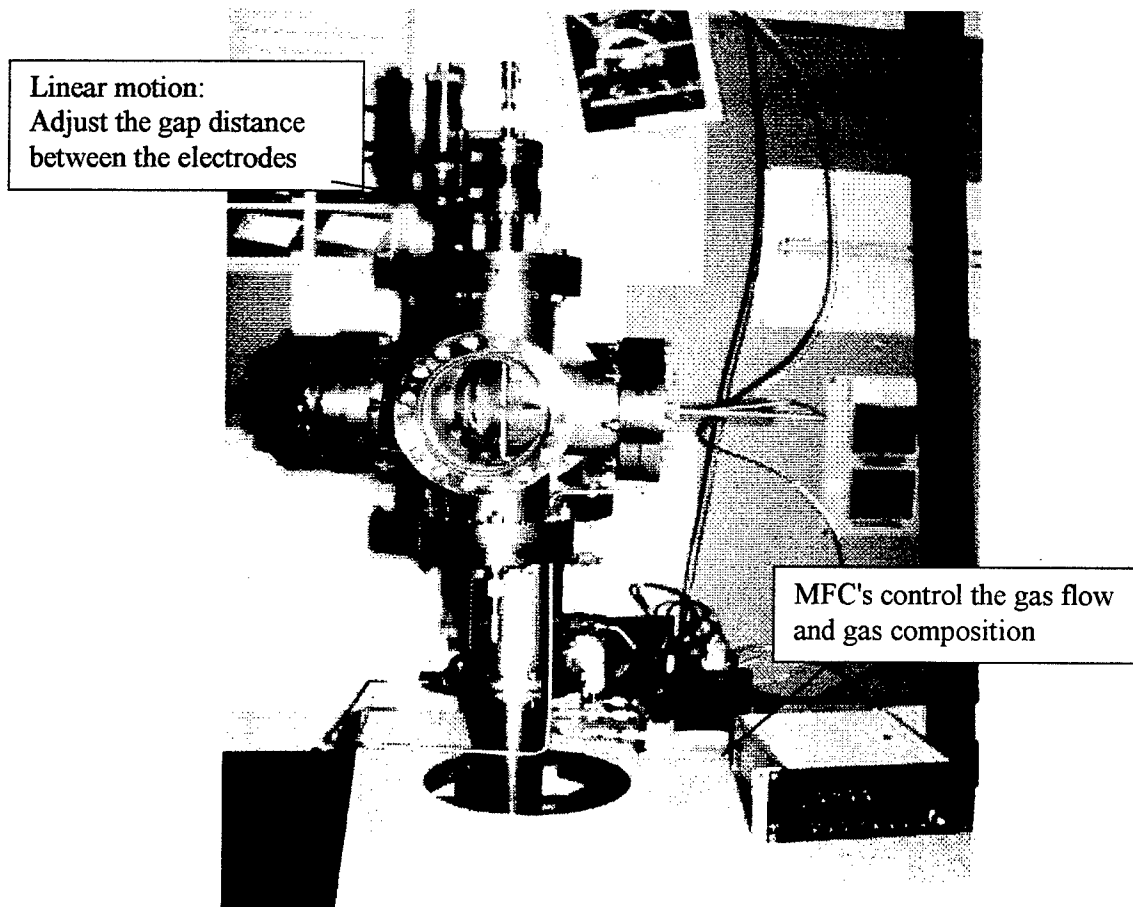


Fig. 5-1 Photograph of CPED test chamber

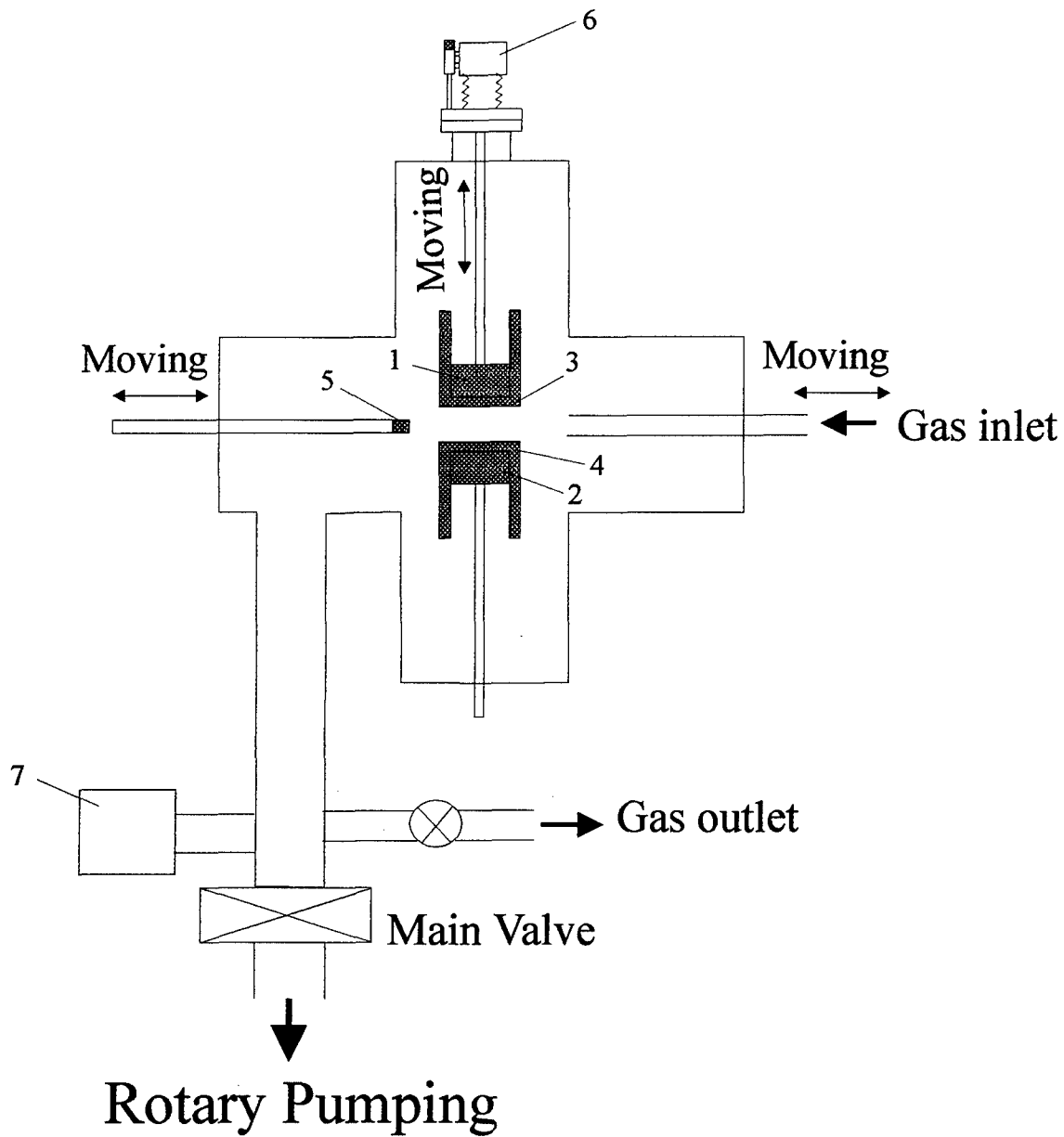


Fig. 5-2 Schematic diagram of Fig. 5-1 for a test beam source system of an atmospheric pressure discharge: 1, Upper electrode 2, lower electrode; 3 and 4, insulator; 5, Langmuir probe; 6, linear motion manipulator; 7, Pressure gage.

A schematic diagram of the CPED system is represented in Fig. 5-2. The equipment was composed of a mechanical pumping system and a linear motion manipulator in order to move the upper electrode, in order to test the effects of various distances between upper and lower electrodes. Also, a gas inlet tube was installed with the capability of linear motion. The system pressure can be controlled from 10 mTorr to 760 Torr by adjusting a manual gate valve and the flow rates of the working gases. Three mass flow controllers (MFC) are used for the gas introduction. In Fig. 5-2, the material of number 1 and 2 is aluminum electrode with 1.55" diameter, and 3 and 4 is ceramic insulator with 2" diameter. A dielectric plate (2" in diameter, 0.0192" in thickness and material: alumina) was used.

Test the HPGD systems: The pressure, pressure gauging and gas introduction were calibrated prior to the discharge test. Pressure calibration curves were obtained for Ar, Air, and other gases. The MFC controlled gas manifold was also tested. One can control the flow of three different gases.

Capacitance: Table 5-1 shows the capacitance between two dielectric shielded electrodes.

Table 5-1. Capacitance between two dielectrics shielded electrodes in an He gas at 1 atm pressure.

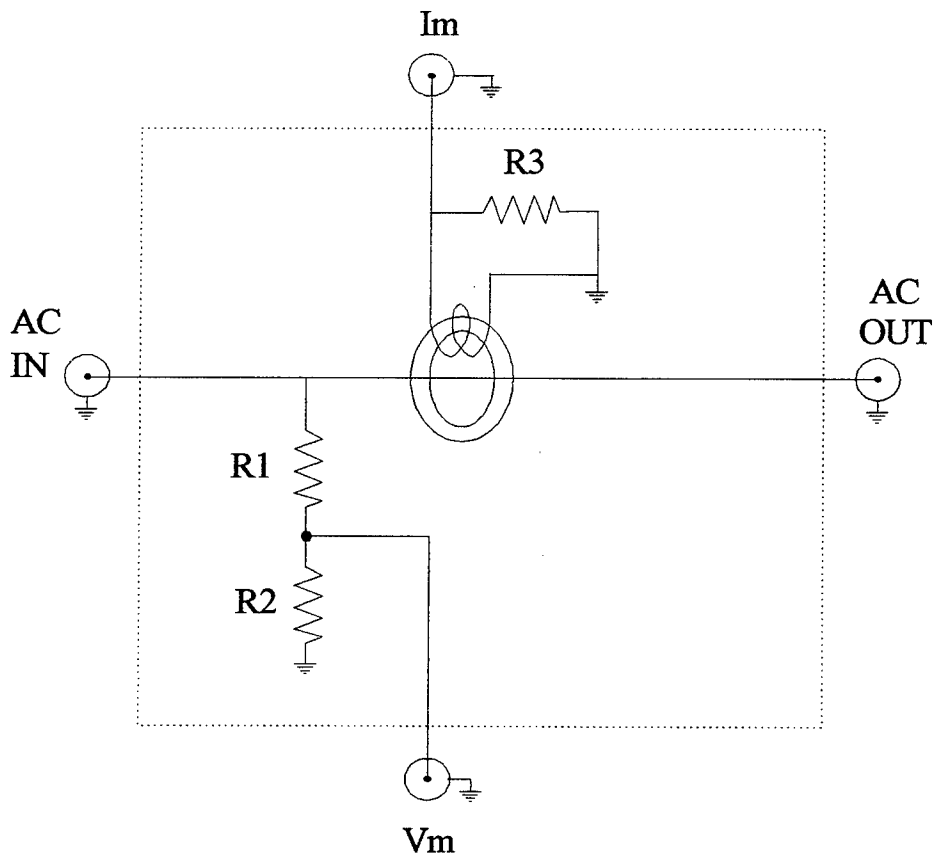
Distance (mm)	0	1	2	3	4	5	6	7	8
C (pF)	62	51	45	42	41	40	40	39	39

Impedance: The impedance under ac voltage is:

$$|Z| = [R^2 + (\omega L - 1/\omega C)^2]^{1/2}$$

The impedance is calculated to be about 400 k Ω at 10 kHz and 5 mm spacing.

I-V characteristics: Fig. 5-3 shows the schematic diagram of the circuit diagram used to measure the I-V characteristics. V_m and I_m are terminals of discharge voltage and current for measurement by oscilloscope.



$$R1 = 3793 \text{ k}\Omega \quad \pm 0.1\%$$

$$R2 = 201 \text{ k}\Omega \quad \pm 0.1\%$$

$$R3 = 100 \text{ }\Omega \quad \pm 1.0\%$$

Fig. 5-3 Electrical circuit for the measurement of the discharge voltage and the current in case of AC.

5-4. Experimental Results

Discharge demonstration: In order to compare our Perforated Electrode Discharge (PED) with other conventional ac-barrier type discharge, we have tested perforated electrode and ac-barrier type arrangement discharge. The complete characteristics of the perforated electrode and ac-barrier type discharge have been analyzed.

Conventional ac-barrier type discharge: First, we reproduced an atmospheric pressure discharge using a conventional ac barrier type arrangement operated in the diffuse mode. Both of the electrodes are covered with dielectric disks. Fig. 5-4 shows the photograph of the discharge made by the ac barrier type at an atmospheric pressure with He gas. The plasma shows stable diffuse mode. RF power and frequency were 150 watts and 10 kHz, respectively.

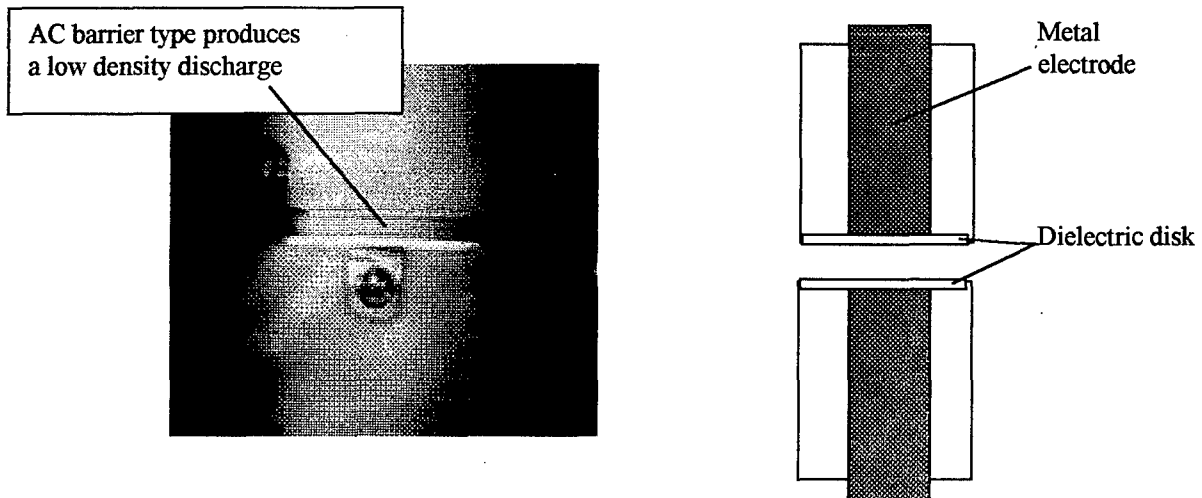


Fig. 5-4 Photograph of an atmospheric pressure ac barrier discharge and schematic diagram.

As shown in Fig. 5-5, the peak voltage is about 500 V and the peak current is about 0.5 A. That is order of magnitude higher than those reported earlier. [9,10] The current peak is shown to start at 150 V which is also lower than Decomps et al. [10]

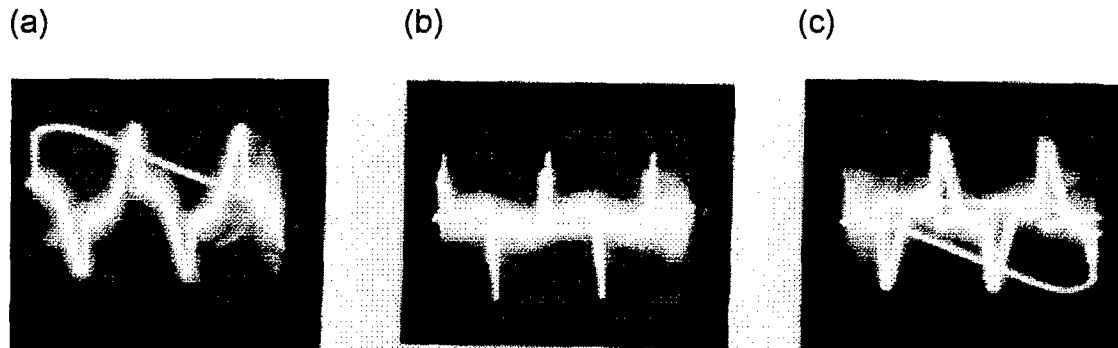


Fig. 5-5 I-V characteristics of AC barrier discharge: (a) applied voltage, (b) discharge current, and (c) I-V

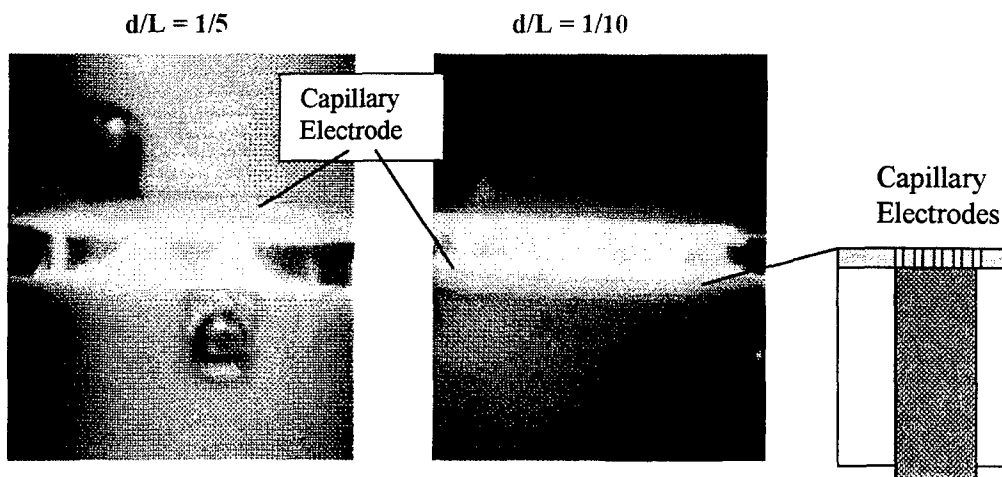


Fig. 5-6 Photograph of an atmospheric pressure Capillary Plasma Electrode Discharge.

CPED discharge: We have also demonstrated CPEG atmospheric discharge as shown in Fig. 5-6. For same conditions as that in Fig. 5-4, a significantly higher density discharge is produced from the capillary electrode. We made two different d/L ratio ($1/5$ and $1/10$) capillary electrodes. In this experiment, mixtures of He and air are used and the chamber is balanced to atmospheric pressure through an open vent hole. The output voltage of the power source we have been using is 500V peak to peak.

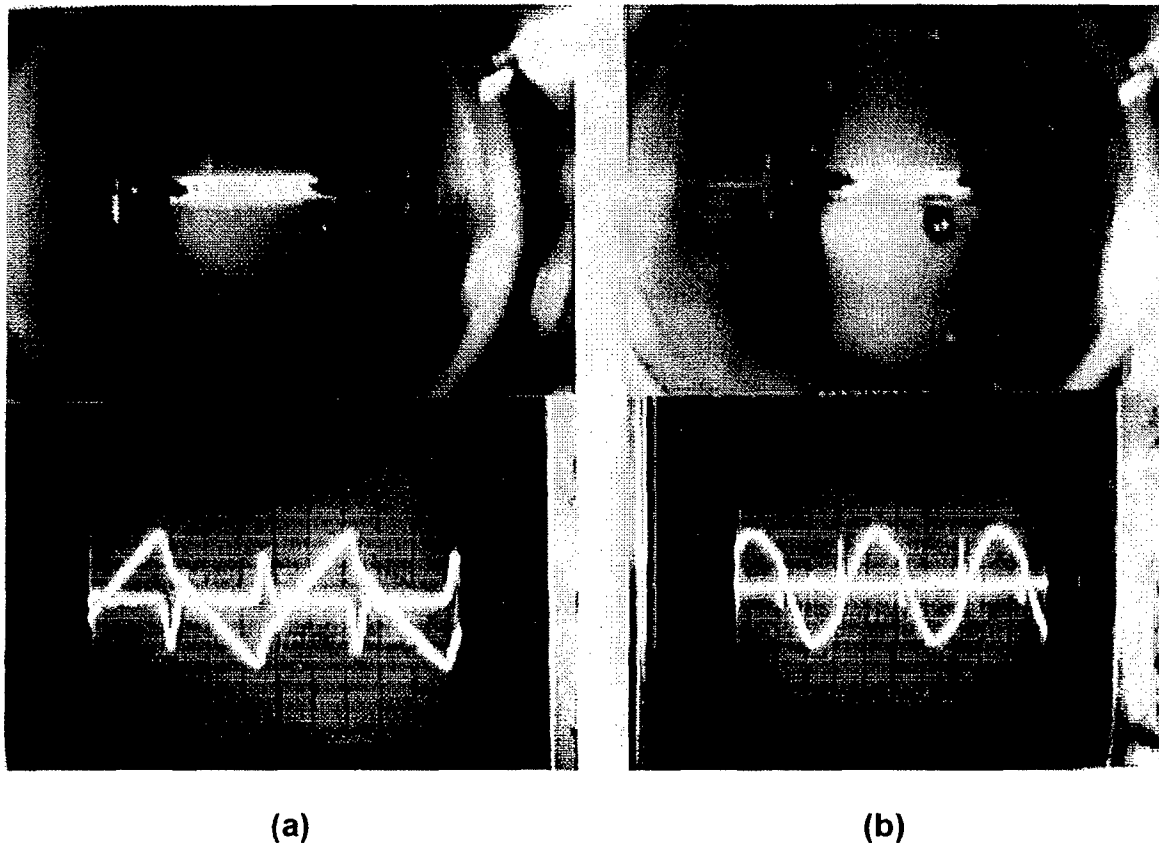


Fig. 5-7 Photographs of micro and diffuse mode glow plasmas made using $f=100$ kHz (a) and $f=15$ kHz (b) in Al_2O_3 /Perforated dielectric of $\phi=0.89$ mm. The oscillograms shown are of the applied voltage and current in each case.

Dependence of frequency and electrode type: We have investigated the discharge characteristics as functions of frequency and voltage for various types of barrier dielectric plates. We used two types of perforated alumina dielectric plates which have ten (10) perforated holes with diameters of 0.89 mm and 0.5 mm and the same thickness of 3.2 mm. The discharge characteristics are compared with non-perforated dielectric plates which have a thickness of 0.488 mm (Al_2O_3) and 1.0 mm (Glass), respectively. The distance between electrodes was fixed to 5 mm.

Table 5-2. The plasma mode state by various electrode type and frequency.

Case of	Capillary or Micro mode			Diffuse mode			Electrode Type
	f (kHz)	V_{pp} (V)	Mode State	f (kHz)	V_{pp} (V)	Mode State	
Fig. 5-7	100	± 200	Capillary	15	± 800	Diffuse >> Capillary	Al_2O_3 /Perforated dielectric. of $\phi=0.89$ mm
Fig. 5-8	100	± 200	Capillary >> Diffuse	20	± 750	Diffuse	Al_2O_3 /Perforated dielectric. of $\phi=0.50$ mm
Fig. 5-9	100	± 200	Capillary << Diffuse	50	± 400	Diffuse	Perforated dielectric of $\phi=0.50/\phi=0.89$ mm
Fig. 5-10	100	± 200	Micro	20	± 1500	Diffuse	Metal (Al)/Glass

Figure 5-7 represents capillary and diffuse mode of glow discharge plasma at frequency $f=100$ kHz (a) and $f=15$ kHz (b) between Al_2O_3 and perforated dielectric of $\phi=0.89$ mm in He gas at one atmosphere pressure. In Fig. 5-7 (a), the plasma spouts out flames with a trumpet-shape from the capillary holes, which forms a stable capillary mode glow discharge. The plasma density in this mode is significantly higher than that of the diffuse mode. The voltage in the oscillogram photograph shows a saw wave form and peak-to-peak voltage

(V_{pp}) of ± 200 V. In Fig. 5-7 (b) with a different frequency of 15 kHz, the plasma is mostly in a diffuse mode with a few weak capillary modes. The plasma mode was varied simply by change of frequency. The voltage is $V_{pp} = \pm 800$ V and shape of a sine wave. The waves of voltage were distorted at the position of current peaks as shown in Fig. 5-7 (b). This means that discharge is generated at this voltage. The voltage was about ± 450 V at the current peak. The experiment results were summarized in Table 5-2. The plasma density in this case is lower than that of the capillary mode (Fig. 5-7 (a)) in spite of higher discharge voltage.

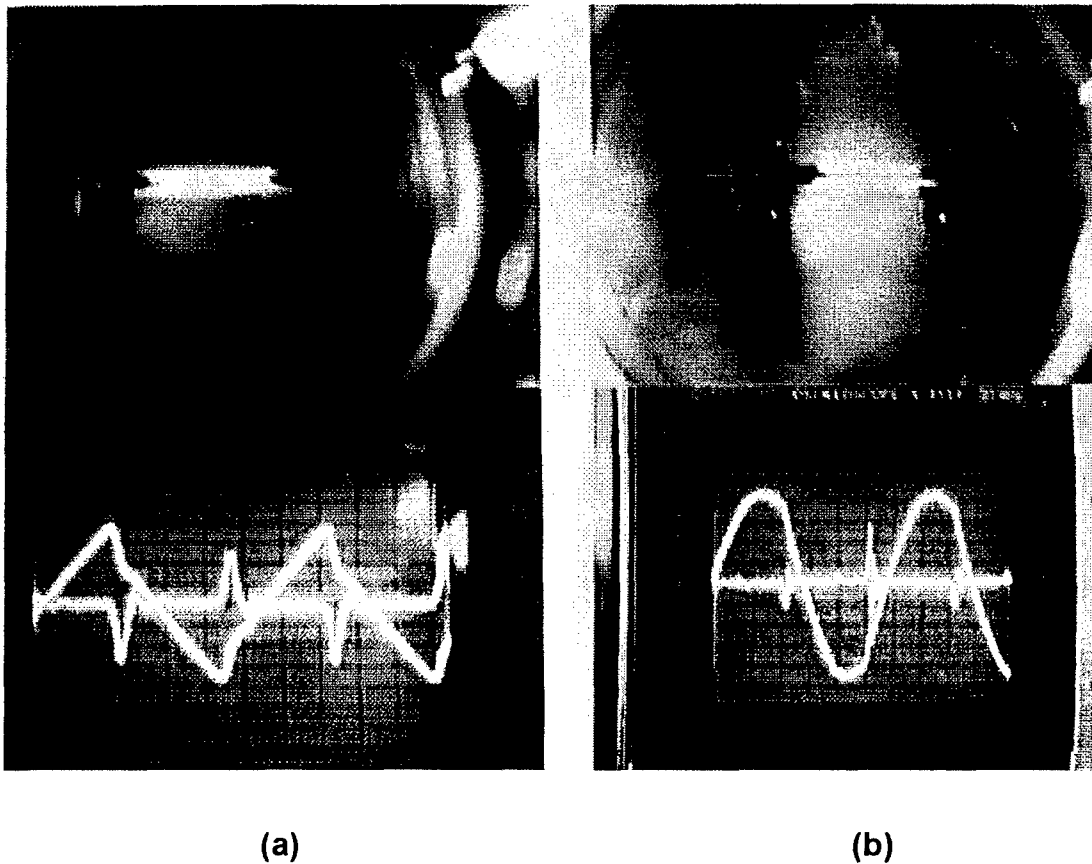


Fig. 5-8 Photographs of micro and diffuse mode glow plasmas made using $f=100$ kHz (a) and $f=20$ kHz (b) in Al_2O_3 /Perforated dielectric of $\phi=0.50$ mm. The oscillograms shown are of the applied voltage and current in each case.

Figure 5-8 shows photographs of glow plasma when the diameter of the hole is $\phi=0.50$ mm smaller than in the case of Fig. 5-7. In Fig. 5-8 (a), the state of plasma was a combination of a high density capillary mode and a low density diffuse mode. The other result was similar to that of the case of Fig. 5-7 (a). In the Fig. 5-8 (b), it showed a perfectly diffuse plasma at 20 kHz. The V_{pp} was ± 750 V and the voltage of discharge generated was about ± 700 V in the oscillogram picture.

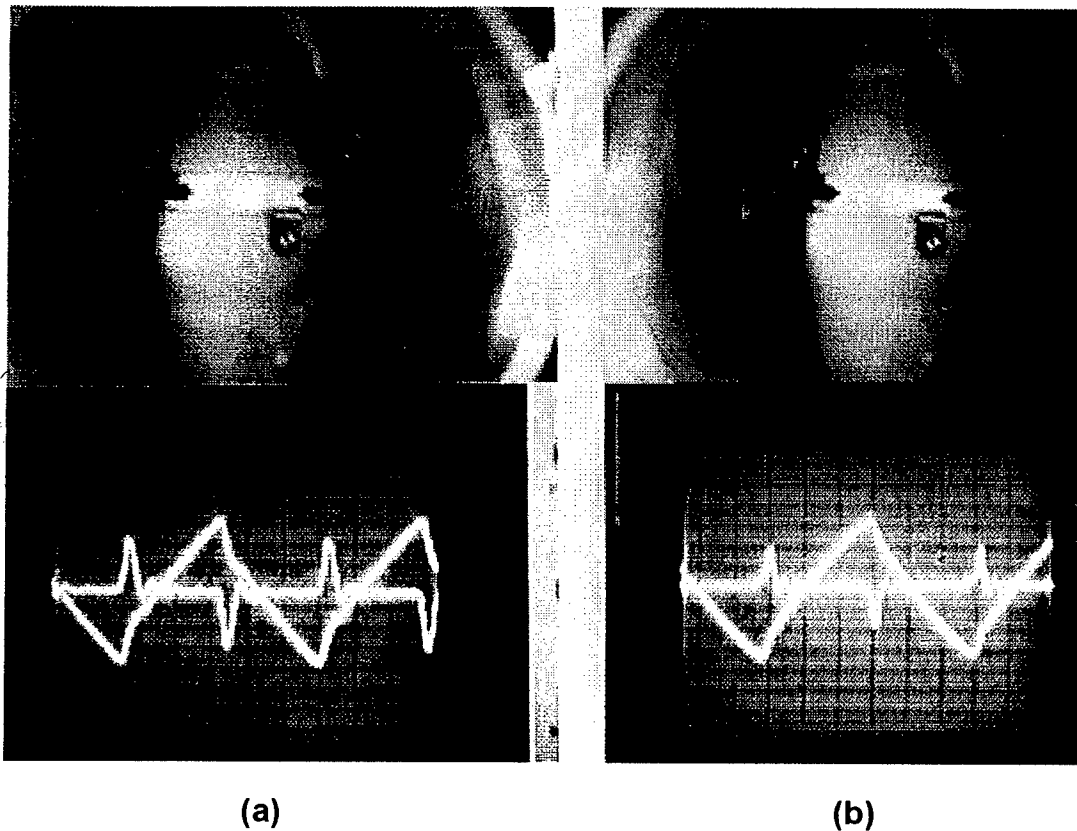


Fig. 5-9 Photographs of micro and diffuse mode glow plasmas made using $f=100$ kHz (a) and $f=50$ kHz (b) in Perforated dielectric of $\phi=0.50$ mm/ $\phi=0.89$ mm. The oscillograms shown are of the applied voltage and current in each case.

In Fig. 5-9, we have tested the perforated dielectric plates on both sides of the electrode. Capillary mode plasma is partially shown mixed with a diffuse mode. In Fig. 5-9 (b), the plasma is wholly in a diffuse mode at the frequency of 50 kHz. The shape of the voltage phase in the oscillogram was a saw wave, different in front, and the V_{pp} was ± 400 V.

Figure 5-10 shows the discharge for an aluminum electrode and glass electrode. The plasma of strong and many micro modes were observed in Fig. 5-10 (a). But, the micro plasma is not stable and is moving around. In Fig. 5-10 (b),

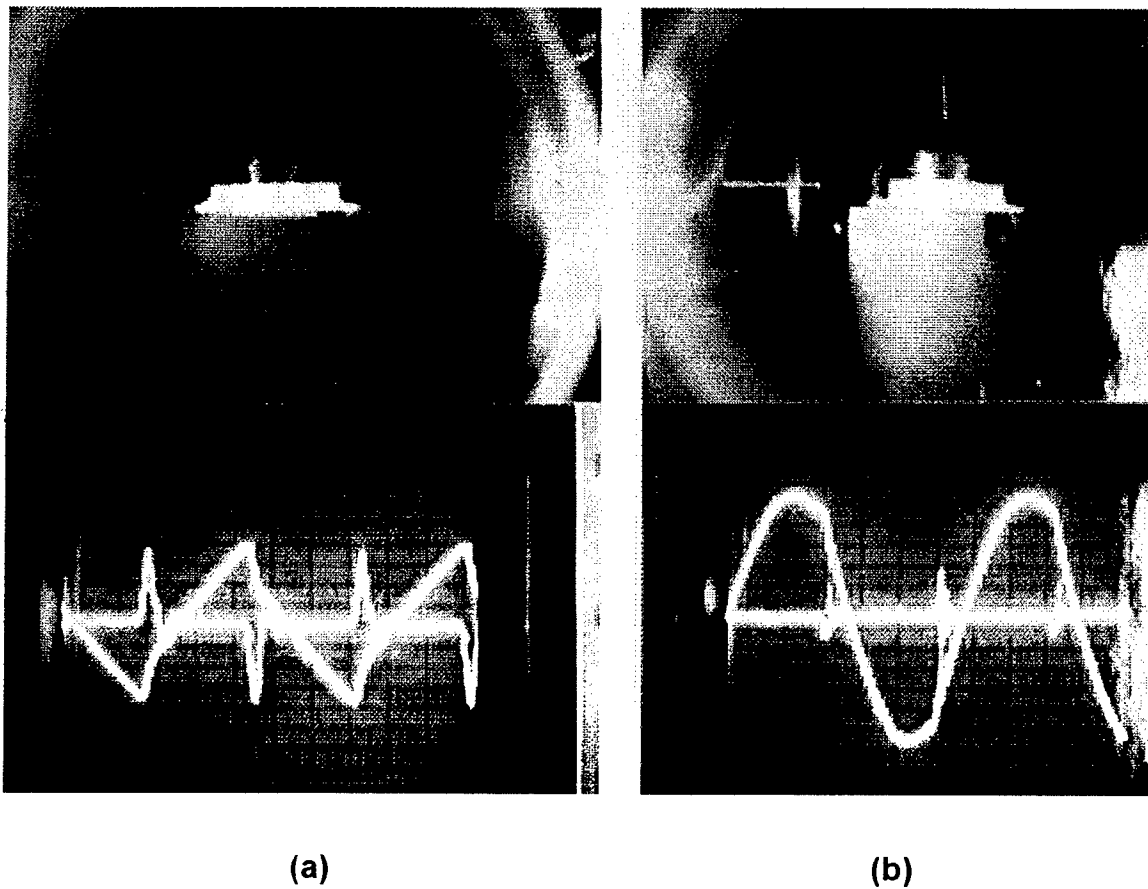
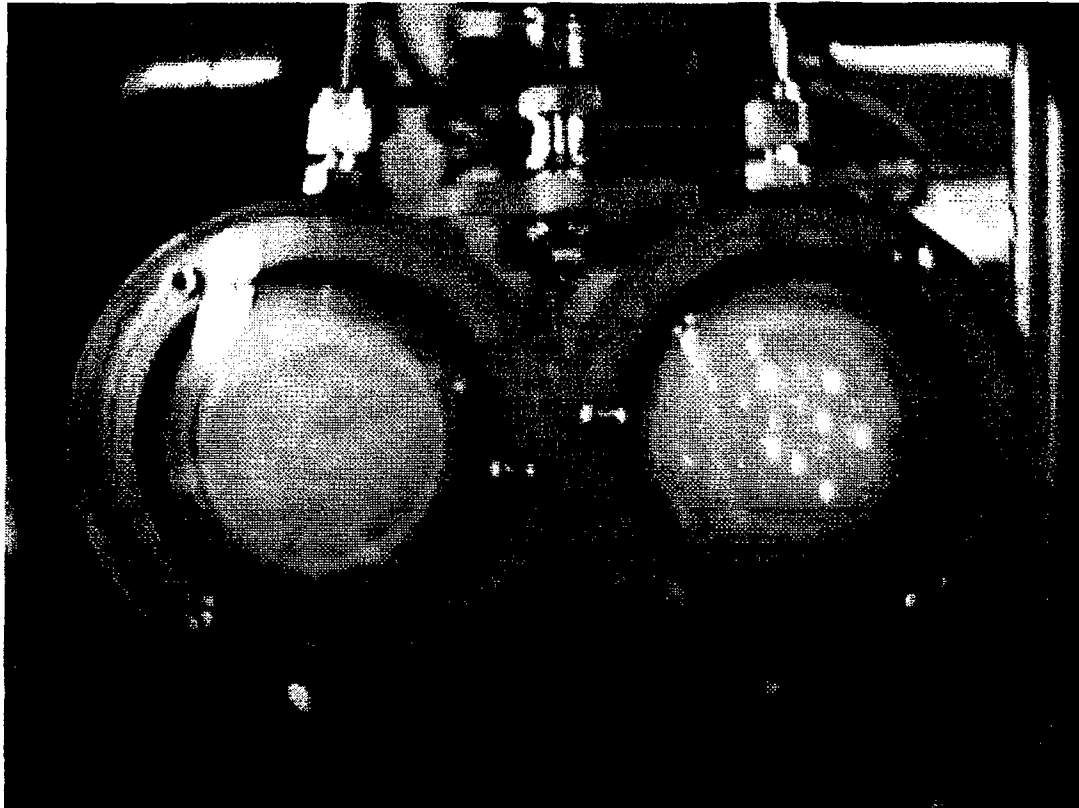


Fig. 5-10 Photographs of micro and diffuse mode glow plasmas made using $f=100$ kHz and $f=20$ kHz (b) in Metal(Al)/Glass. The oscillograms shown are of the applied voltage and current in the each case.

plasma at a frequency of 20 kHz was a perfected diffuse mode. The V_{pp} was ± 1500 V, higher than the other case, and the plasma generation voltage was about ± 1300 V. All the experiments were performed at atmospheric pressure.



(a)

(b)

Fig. 5-11 Top view photographs of (a) diffuse mode in dielectric electrode and (b) capillary mode plasma in CPED.

Plane view of capillary and diffuse mode plasma: Figure 5-11 shows top view photographs of generated plasmas; (a) is an already well-known diffuse mode plasma and (b) is a plasma of capillary mode invented by Erich Kunhardt and Steven Kim. The pressure is atmospheric pressure and the gas used is Helium. The voltage and frequency applied to both systems was 400 V and 100 kHz. The

appearance of the plasma in (b) has bright spots around the holes of the dielectric electrode, which differs from the silence and uniform plasma in (a). The intensity of plasma in the spots is higher than that in (a), hence the plasma produced by the capillary plasma electrode discharge (CPED) is expected to be more effective for sterilization of bacteria than the diffuse mode plasma.

CPED system test for portability: We made and investigated various high pressure glow discharge arrangements suitable for a portable CPED system.

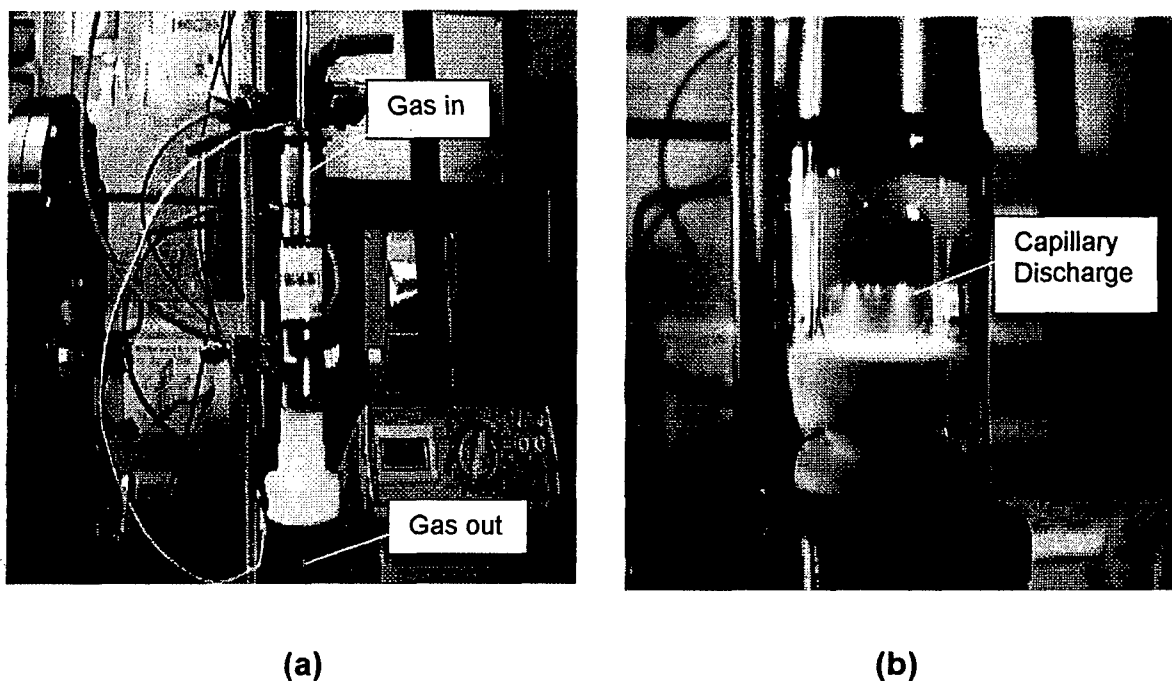


Fig. 5-12 Photographs of portable CPED system of small size (a) whole system, (b) zoomed view for discharge injection.

Figure 5-12 represents (a) the whole portable CPED system and (b) the discharge plasma in one atmospheric pressure of He gas. In the system, the upper electrode is a perforated machinable ceramic with 7 holes. The thickness and diameter of the hole are 1.5 mm and 0.7 mm, respectively. The lower

electrode is dielectric (machinable ceramic) with 2 mm thickness. The optimum frequency for capillary discharge generation was about 28 – 34 kHz. The difference from the previously reported frequency is due to the fact that the dimensions of this system are different. The discharge spouts out from the capillary holes and is a stable capillary mode glow discharge.



Fig. 5-13 Photograph of atmospheric pressure plasma using one capillary tube by 14 kV DC voltage.

Figure 5-13 shows a photograph of the plasma from one capillary when the voltage is 14 kV DC. The diameter and length of the capillary is 1.0 mm and 50 mm, respectively. The ignition voltage for the plasma was about 14 kV, which is significantly higher than 400-800 V AC reported in Fig. 5-4 ~ 12. The discharge is still cold plasma.

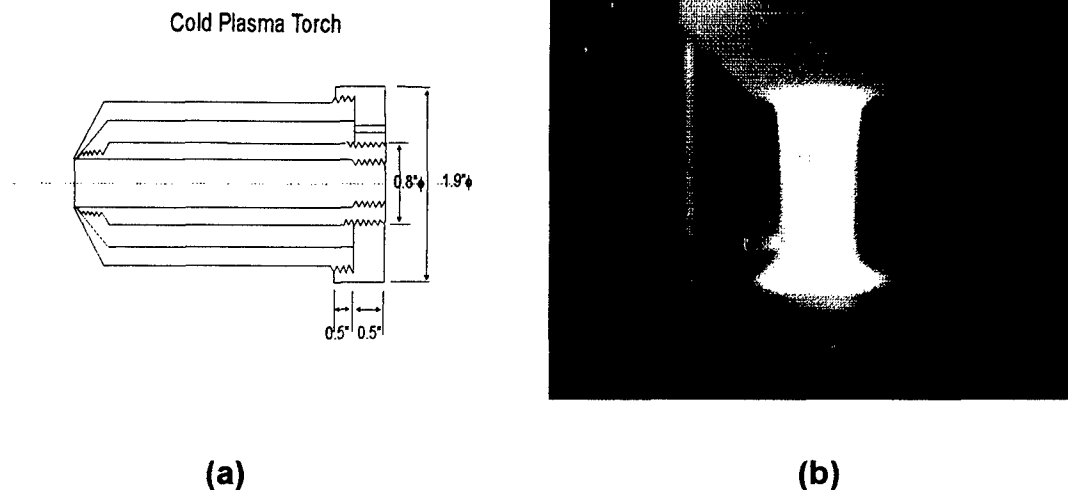


Fig. 5-14 Schematic diagram of the portable cold plasma torch (a) and photograph of the plasma (b).

A schematic diagram of a portable cold plasma torch and photograph of the plasma are shown in Fig. 5-14. In (a), the diameter of beam was designed to be 0.5 inch, material of the case was made of Teflon and a perforated dielectric was not used. The applied voltage was 3 kV AC and the frequency was 33 kHz. In (b), the plasma state showed a stable and uniform diffuse mode. However, the plasma density was not stronger than that of Fig. 5-12 and Fig. 5-13 with capillary mode plasma. The length of the discharge reaches up to 5 cm.

Figure 5-15 shows photograph of cold plasma shower by portable CPED with half-inch diameter. Applied voltage and frequency were about 10 kV and 3 MHz, respectively. The plasma states showed stable and silent capillary mode in an atmospheric pressure of He gas. The plasma density was greater than the diffuse mode plasma in Fig. 5-14. The plasma stream diffuses out to one inch.

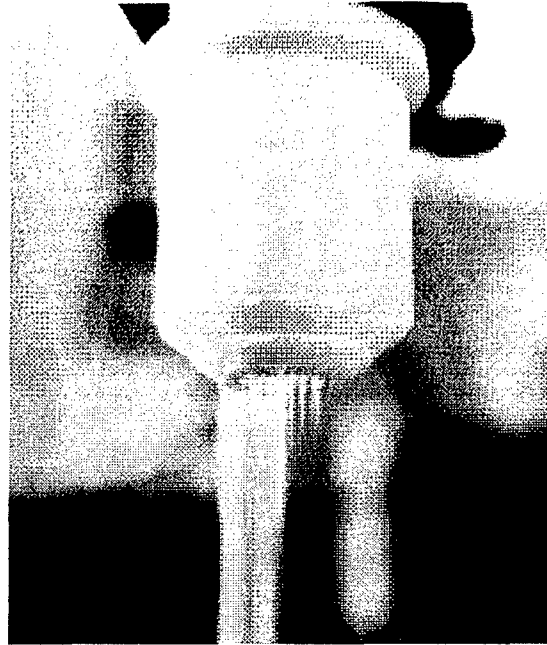


Fig. 5-15 Photograph of portable CPED shower with ½ inch beam diameter.

Decontamination Test:

We have demonstrated the decontamination capability by subjecting samples to conventional ac barrier type discharge and CPED discharge. A soil sample was suspended in water and filtered to remove debris. A spore stain of a sample (0.1 ml) smeared and fixed to a microscope slide confirmed that endospores were present. The sample included water was dried in air. Two experiments were performed. In the first experiment, a loopful of the suspension was applied directly into the chamber. The sample was then subjected to continuous ac barrier type (in Fig. 5-4) or CPED radiation (in Fig. 5-6) for 5 minutes at power 100 W. The treated sample was collected onto a cotton swab, wetted with sterile distilled water. The cotton swab was submerged into 1 ml of sterile distilled water. The swab was then streaked onto LB agar plates (yeast extract and tryptone), and incubated at 37°C for 18 hours. Any resultant lawn of microbial growth was observed as shown in Fig. 5-16 (c). A positive control that

was not treated with radiation was included. The degree of lawn growth was reduced with diffuse radiation, but a large amount of microbial growth was observed as shown in Fig. 5-16 (b). In sharp contrast, only a single bacterial cell survived the capillary method of treatment; there was not lawn of microbial growth as shown in Fig. 5-16 (a). The single bacteria cell is believed introduced after the treatment while we are handling the samples.

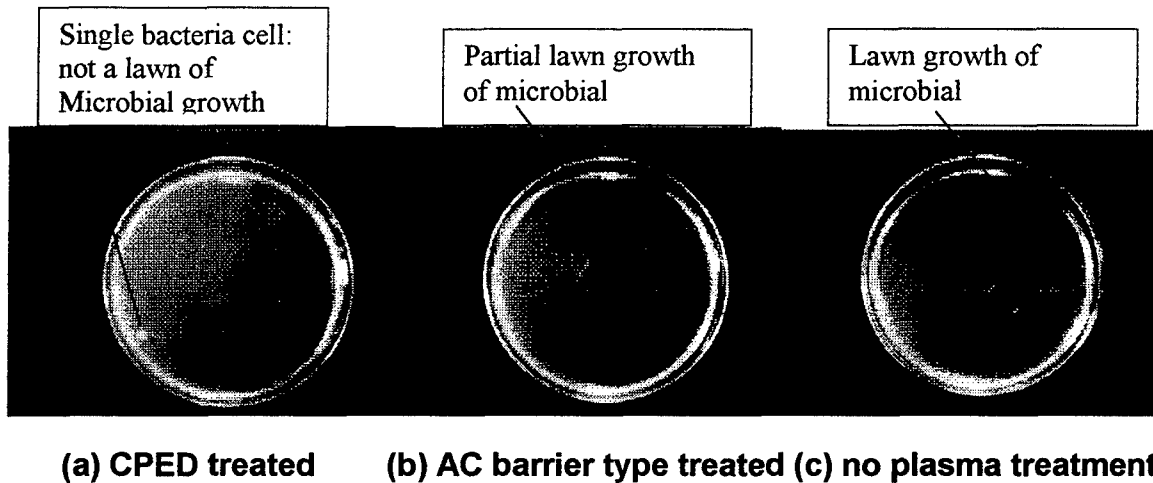


Fig. 5-16 Lawn growth of microbial onto LB agar plates: (a) CPED treated: no lawn growth is observed, a single bacterial cell is observed which may be introduced while we are swabbing after the treatment (b) AC barrier type treated: 1/3 of lawn growth is observed compare to no plasma treated sample, (c) lawn growth image of no plasma treated sample.

In Fig. 5-16 (b), we observed traces of growth in the upper part as germs propagated. An optical microscope image for this region is shown in Fig. 5-17 (b), where B is a bacterium. Figure 5-17 shows optical microscope image of microbial growth. Two types of radiation, AC barrier type (in Fig. 5-4) and CPED (in Fig. 5-6), were applied to two separate loopfuls of a sample of microbes and then streaked onto an agar plate. After incubation at 37°C for 18 hours, the

plates were compared for microbial growth. (b) shows microbial growth spreading out from the streak lines; this sample was treated with diffuse radiation. It is apparent in (a) that no such growth occurs from the streaked sample that was treated with capillary radiation.

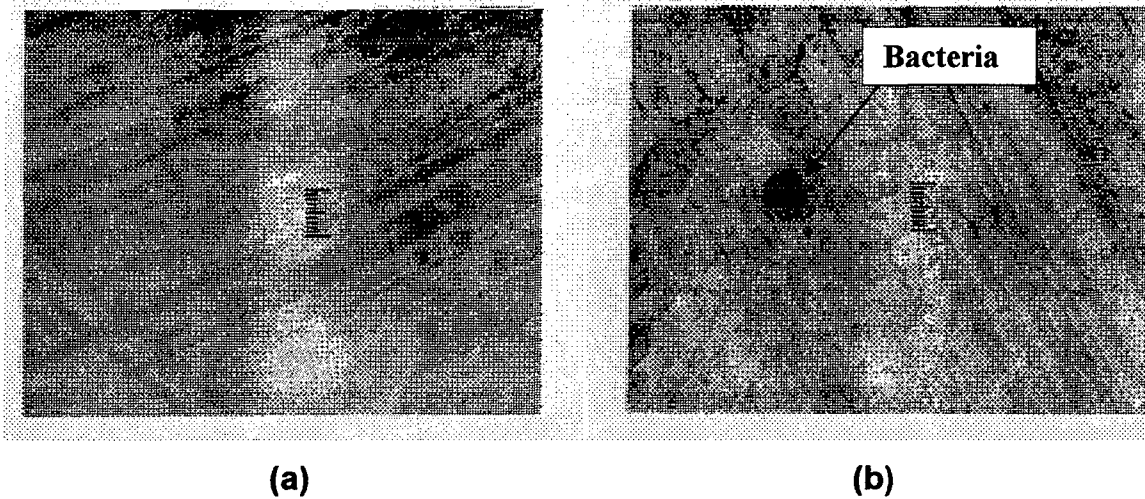


Fig. 5-17 Optical microscope image of microbial growth in Fig.5-16 (a) and (b), respectively, at two types of radiation as CPED (a) and AC barrier type (b).

5-5. Conclusion

A CPED test system was designed and constructed using a vacuum system whose pressure can be controlled from 10 mTorr to 760 Torr, which was equipped with three mass flow controllers (MFC) and a linear motion manipulator. The dimension of the optimum perforated dielectric was investigated by using two different d/L ratio (1/5 and 1/10) capillary electrodes.

By controlling the frequency, we were able to change the discharge mode from a capillary mode (with enhanced plasma density and U-V photon) to diffuse mode (ac barrier type). The capillary mode has been found to be stable in between 70-150 kHz range and with pulsed DC sources. These two discharge modes are functions of pressure, frequency and voltage. Dielectric and perforated dielectric pair (a perforated dielectric has a hole diameter of 0.9 mm and a thickness of 3.2 mm) was found to produce the most stable high density capillary mode discharge. Also, we designed, made, and tested various portable HPGD systems and a portable CEDP shower with 1/2" beam size. The applied frequency was varied with the dimension of the system to produce the most suitable plasma.

We investigated the treatment of bacteria by capillary and diffuse plasmas. Perfect pasteurization of bacteria was only possible using the capillary mode plasma, despite the fact that the power used was much lower than that of the diffuse plasma. This demonstrates that only the capillary effect plasma, proposed and developed by our group, is successful in pasteurization.

6. Phase II Plan

Overview

The Phase II effort has three major objectives

1. **Refine the process technology:** One of the key elements in the performance of the CPED is the d/L ratio of the capillary. We will investigate the behavior of capillaries with ratios from 1/10 to 1/100. The operational variables for the process are pressure, frequency, voltage and electrode gap. We will optimize the process varying frequency, voltage and gap at atmospheric pressure. We will construct a new 6" diameter electrode chamber for the optimization study. The new chamber will have a new capability for monitoring the discharge distribution from the top view port.
2. **Construct a portable 6" CPED Shower:** Based on optimized conditions for the CPED structure, we will construct a portable CPED Shower. We will build two Shower heads: one for pulsed DC/DC and the other for AC operation.
3. **Field work of decontamination:** In collaboration with Prof. Carol Stone, Chemistry Department at Stevens, we will investigate the decontamination capability of PLASMION's CPED Shower. After laboratory test at Stevens, we will perform a field test at the contractor facility – simulated battlefield chem/bio hazard environment.

The power supply for CPED will be developed in collaboration with Advanced Energy Industries Inc. The Advanced Energy is one of the leading US manufacturers of power supplies for plasma assisted semiconductor processing.

Their participation will greatly enhance this program. The portable 6" CPED Shower will be powered by a motor vehicle.

Refine the process technology

A test system is very important for us to refine the process technology and develop an optimum CPED Shower structure.

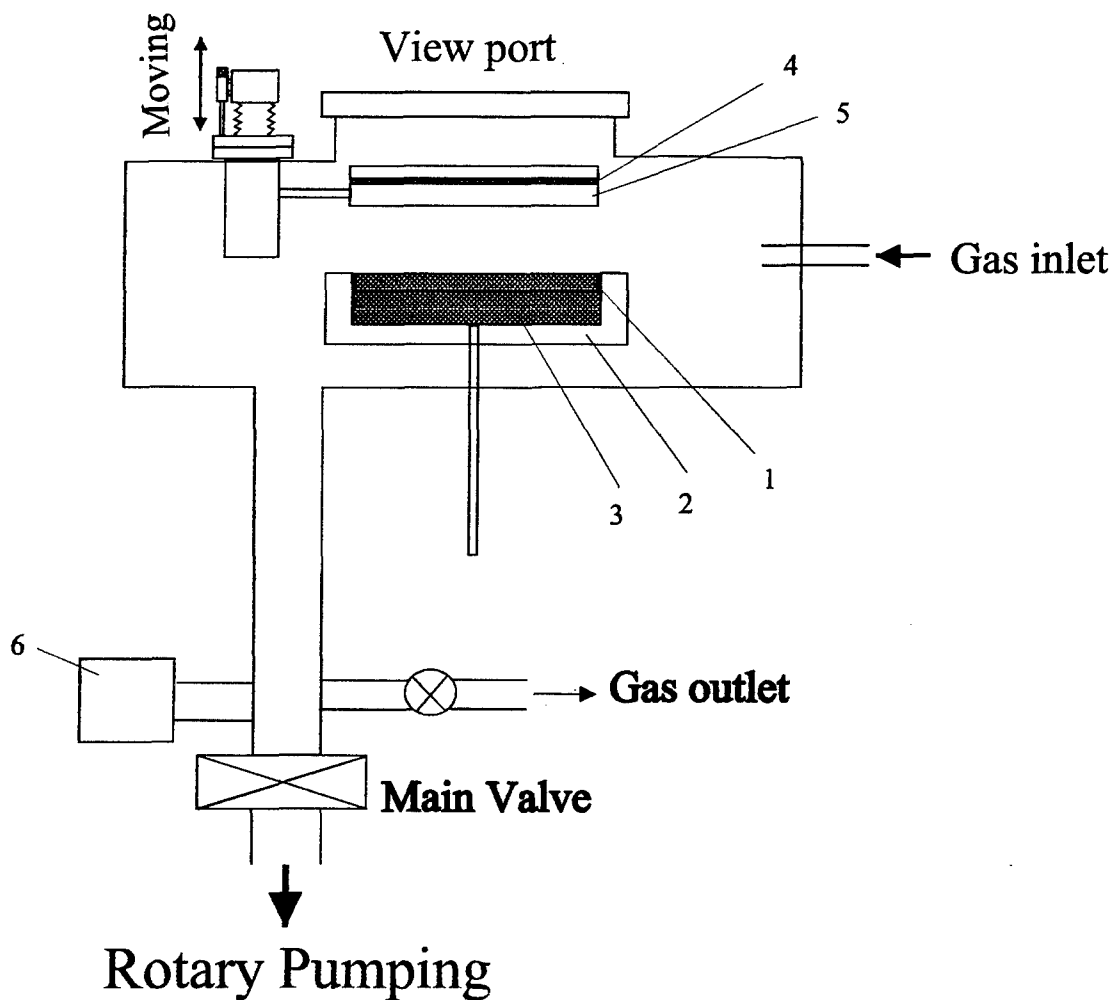


Fig. 6-1 Schematic diagram of large area CPED test beam source system: 1, Capillary dielectric; 2, insulator; 3, lower electrode; 4, ITO; 5, Glass; 6, Pressure gauge.

Schematic diagram of a 6-inch area CPED test beam source system is shown in Fig. 6-1. The test system is very important for us to refine the process technology and develop an optimum CPED shower structure. Several new features will be added compared with our phase I using 2" electrode test chamber. We will make a transparent upper electrode using an ITO coated electrode as schematically shown in Fig. 6-1. Through this view port, we will be able to monitor the uniformity and spectra of the discharge. As seen in our previous photo, the capillary discharge beam diverges from the exit capillary. The cross section spectral image of the discharge will be investigated and we will refine the process to make a uniform beam cross-section. Also, the gas spectra will provide important information on radical production and lifetime. At Stevens, we have a high speed frame camera and we will be able to investigate the time variation of the radical spectra.

We will prepare the side port to simulate the actual field application. In the field application, there will be a windy situation. The blower is mounted on the side port and the discharge stability and uniformity will be investigated. We will find the optimum parameter to compensate for the wind effect.

Construct a portable 6" CPED Shower

For the battlefield decontamination application, a spray type plasma structure is suitable rather than a diode type. The versatile structure of CPED allows us to develop a spray type discharge tool. The capillaries act as a gas channel where the radicals, ions, and electrons are produced. The flow stream will provide a longer mean free path for the radicals. In our Phase I, we demonstrated the feasibility of the CPED shower as shown in Fig. 5-14 and 15. PLASMION's CPED Shower is the world's first non-thermal plasma spray demonstrated at atmospheric condition. We will develop a 6" CPED Shower in Phase II. Based on our Phase I work, both AC and DC are feasible. AC arrangement would be beneficial for the convenience of the operation at lower voltages, however, DC operation may have a better capability of radical production and a higher duty cycle. We plan to pursue our investigations with

both types of operation since at this time we have not determined which approach is overall better suited for killing all forms of spore forming bacteria. Thus, we will investigate both AC and DC operation in Phase II.

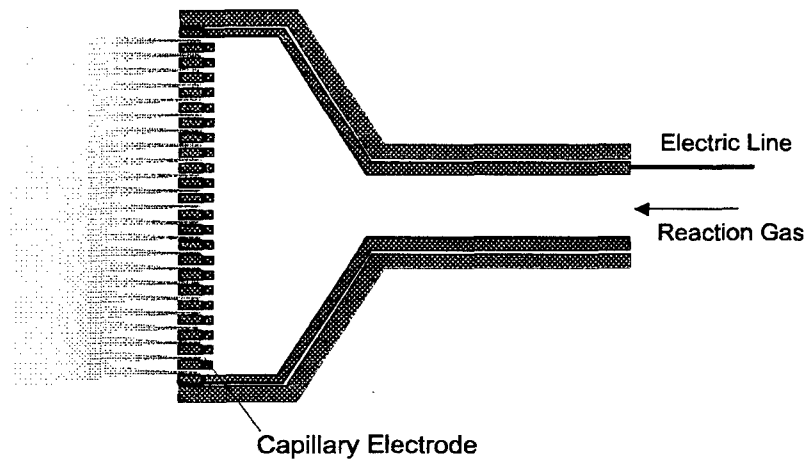


Fig. 6-2 Schematic presentation of large area CPED Shower system.

Fig. 6-2 represents schematic presentation of 6-inch area CPED Shower system. For the decontamination application, diode structure is not suitable. We invented a "CPED Shower" for portable decontamination application. We take advantage of the structure of the capillary. The reaction gas is fed from the back. The radical, ions, and electrons are produced in the capillary and diffuse out. Through the stream of the discharge, the radicals are produced due to the collision between ions and electrons. A high AC voltage of 3-15 kV is required for the generation of the plasma stream. The discharge is a non-thermal discharge.

Field work of decontamination

In Phase II, we will develop a portable plasma shower head for battle field decontamination as shown in Fig. 6-3.

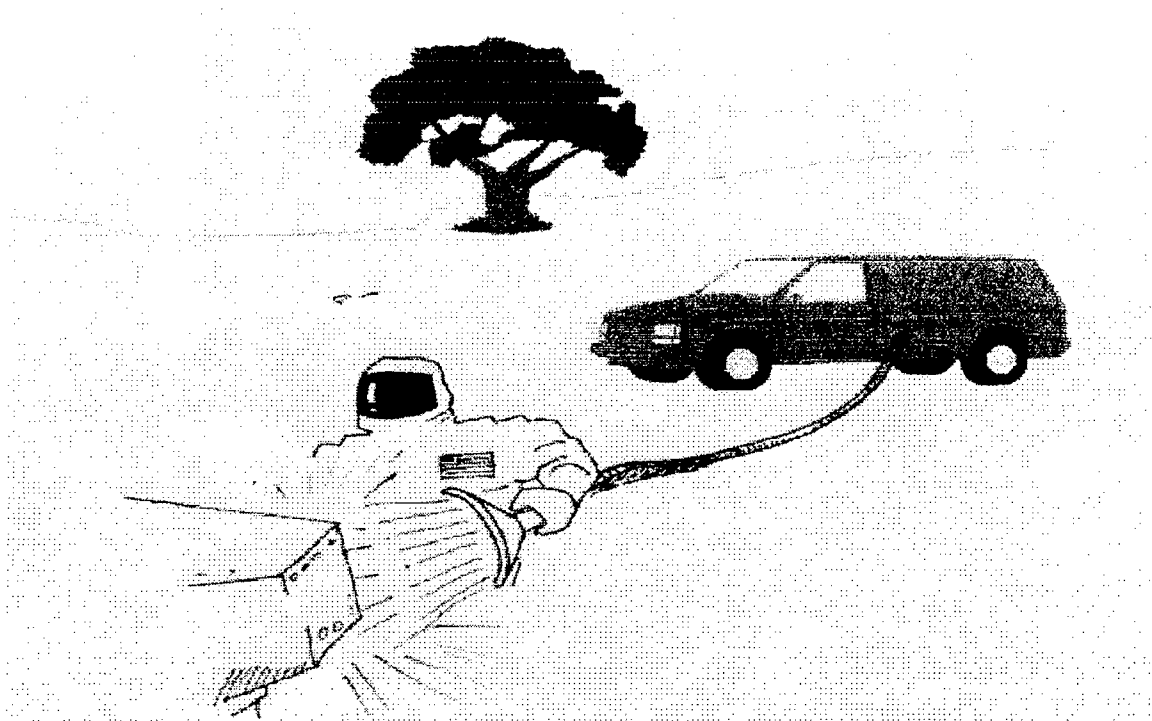


Fig. 6-3 Schematic presentation of CEDP-Shower battle field chem/bio decontamination

Laboratory test: We will test the effectiveness of the capillary method and the developed shower in the laboratory by two techniques. One technique will be performed with spore strips containing *Bacillus subtilis*. The *Bacillus* genus, which also contains the deadly *Bacillus anthracis* bacterium, is often used to test the validity of sterilization conditions. Spores created by this genus are resistant to adverse conditions. The spore strips will be used in experiments with capillary radiation to determine the effectiveness of the radiation. After treatment, the strips will be cultured onto petri dishes containing nutrient agar (beef extract and peptone), incubated for 18 to 24 hours at 37°C, and examined for bacterial growth.

The above protocol will be used routinely as the capillary radiation instrument is developed. A variety of surfaces will be used to test the ability of the instrument to penetrate porous surfaces. Plastic, metal, paper, and rubber surfaces will be smeared with *B. subtilis* cultures before treatment with radiation. The surfaces will then be swabbed and streaked onto petri dishes containing nutrient agar, incubated for 18 to 24 hours at 37°C, and examined for microbial growth. Protocols will be developed that stipulate the amount of radiation and the time of continuous radiation necessary to destroy the *B. subtilis* spores.

Once confident that the unit works well with a variety of surfaces, the unit will be tested in the laboratory under controlled conditions with the *B. anthracis* bacterium to confirm that radiation of this species responds similarly to the radiation.

The bacterium *Bacillus subtilis* will initially be used as an indicator of the efficacy of the plasma. This organism is a gram positive rod shaped bacterium with the added ability to form endospores when nutritionally stressed. These spores are extremely resistant to many chemicals and radiation. *B. subtilis* is used in industry to test the efficacy of autoclaves and other sterilization devices, including those using radiation. It is a relatively harmless organism commonly found in soil. It is however, related to the pathogenic *B. anthracis* bacterium that causes deadly anthrax.

Field test: Using *B. subtilis* as the agent of contamination, field experiments with the instrument will be performed to test the mobility of the unit and its effectiveness in the field. The experimental procedure developed in the laboratory will be used in these field experiments. Specifically, a variety of surfaces will be smeared with *B. subtilis* cultures before treatment with the plasma. The surfaces to be contaminated will include those most commonly found in the field, including tires, windshields, gloves, and eye gear. The amount of exposure time will depend on the outcomes of the previous surface experiments conducted in the laboratory.

After treating the surfaces with CPED, those surfaces will be swabbed with sterile cotton swabs and streaked onto petri dishes containing nutrient agar. The plates will be incubated for 18 to 24 hours at 37°C and examined for microbial growth. Plates that do not contain a lawn of microbial growth will be considered successful.

If the field experiments with *B. subtilis* are successful, field experiments with *B. anthracis* may also be performed. The spores produced by the bacterium are pathogens, and controlled conditions will be necessary to performed this experiment. For instance, it will be necessary to limit the amount of anthrax germs carried into the field. Also, the day will be chosen to minimize windy conditions. Also, individuals involved in the experiments will use masks to avoid inhaling the potential pathogen. As with the previous field experiment, various surfaces will be smeared with the bacterium, and then decontaminated with the CPED instrument. The treated surfaces will be swabbed with sterile cotton swabs and the swabs will be streaked onto petri dishes. A lack of microbial growth will indicate that even the most resistant potential pathogens are destroyed by the CPED technique.

7. References

1. Wehrli, M. Z. Phys. **44**, 301 (1927)
2. T. Yokoyama, M. Kogoma, T. Moriwaki, and S. Okazaki, J. Phys. D: Appl. Phys. **23**, 1125 (1990)
3. C. Liu, P. P. Tsai, and J. R. Roth, 20th IEEE Conf. Plas. Sci., Vancouver, BC, Canada, (1993).
4. Yu. S. Akishev, A. A. Deryugin, I. V. Kochetov, A. P. Napartovich, and N. I. Trushkin, J. Phys. D: Appl. Phys. **26**, 1630 (1993).
5. R. J. Vidmar, IEEE Trans. Plasma Science **18**, 733 (1990)
6. Y. P. Raizer, *Gas Discharge Physics*, Springer Verlag, Berlin, 1991, chap 13
7. A. P. Napartovich, Yu. S. Akishev, "Glow Discharge in a Gas Flow: Physics and Applications", XXI intern. Conf. Phenomena in Ionized Gases, Bochum, Germany, 1993, Proc. III, p.207)
8. F. Massines, R. B. Gadri, P. Decomps, A. Rabehi, P. Segur, and C. Mayoux, American Institute of Physics, 306 (1996)
9. T. Yokoyama, M. Kogoma, T. Moriwaki, and S. Okazaki, IOP Pub., Rapid Communication, 1125 (1990)
- 10 Ph. Decomps, F. Massines, and C. Mayoux, Acta Phys. Universitatis Comenianae **35** (1), 47 (1994)